

Supplementary material

Ultralong-lifetime Ti/RuO₂-IrO₂@Pt Anode with Strong Metal-Support Interaction for Efficient Electrochemical Mineralization of Perfluorooctanoic Acid

Jianjun Zhou^a, Tian Wang^a, Cheng Cheng^a, Fan Pan^a, Yunqing Zhu^{a,*}, Hongrui Ma^a, and
Junfeng Niu^{a,b,*}

^a School of Environmental Science and Engineering, Shaanxi University of Science and
Technology, Xian 710021, PR China

^b School of Environment and Civil Engineering, Dongguan University of Technology,
Dongguan 523808, PR China

* Corresponding author.

E-mail address: zhuyunqing@sust.edu.cn (Yunqing Zhu); niujf@dgut.edu.cn (Junfeng Niu)

Further Material Characterizations:

Text S1. Electrode preparation

Fig. S1. Contact angle photograph of Ti/RuO₂-IrO₂@Pt (a), Ti/RuO₂-IrO₂-Pt (b), and Ti/RuO₂-IrO₂ (c).

Fig. S2. The elemental composition of Ti/RuO₂-IrO₂@Pt (a) and Ti/RuO₂-IrO₂-Pt (b) electrodes.

Fig. S3. CV curves of Ti/RuO₂-IrO₂@Pt (a), Ti/RuO₂-IrO₂-Pt (b), and Ti/RuO₂-IrO₂ (c) electrodes at different scanning rates. The electric double-layer capacitance diagram of these electrodes (d).

Fig. S4. Electrochemical degradation of actual pharmaceutical wastewater (obtained from Hebei pharmaceutical factory in China). (a) Chemical oxygen demand (COD) and (b) color changes with the time of electrolysis. (c) Continuous experiment by using Ti/RuO₂-IrO₂@Pt anode.

Fig. S5. ESI mass spectrum of the PFCAs by using UPLC-MS/MS.

Table S1. Comparison of service life of different DSA anodes.

Table S2. Comparison of PFOA degradation using DSA or BDD anodes.

Text S1. Electrode preparation

Ti plates were cut into pieces of 8 cm × 12 cm and pre-treated by polishing, degreasing, acid-etching, and ultrasonic cleaning, then dried in nitrogen before applying catalysts. During the degreasing process, the plates were immersed in acetone and ethanol solution with ultrasonic for 10 min. The plate was then acid-etched using 10% oxalic acid in a water bath at 80 °C for 2 h to polish its surface chemically. The pre-treated Ti plates were stored in an ethanol solution until use.

Preparation of the Pt/Ru-Ir oxide catalysts with the modified microemulsion method and electrode calcination is described as follows. Firstly, CTAB was added to an intensely stirred C_7H_8 solution to form an evenly dispersed suspension, the Pt precursor solution containing $H_2PtCl_6 \cdot 6H_2O$ was then added to the above suspension, and stirred overnight. Secondly, the Ru and Ir precursor solution containing $RuCl_3 \cdot 3H_2O$ and $IrCl_3 \cdot xH_2O$ was added into the suspension prepared in the first step and stirred for 30 min, then excessive NaOH solution was added and stirred evenly. The resulting microemulsion mixture was centrifuged and collected, and then dried overnight at 105 °C. Thirdly, the dried sediment was ground into powder and added into C_3H_8O solution in a round-bottom flask, and the flask was immersed into a thermostatic oil bath with magnetic and stirred at 80 °C for 3 h. Finally, an appropriate amount of the above coating solution was evenly painted on the pre-treated Ti substrate, then the produced electrodes were dried at 80 °C for 10 min, and the above steps were repeated several times. Lastly, the coatings were annealed in a muffle furnace at 450 °C for 2 h. The Ti/RuO₂-IrO₂-Pt electrode was also prepared as control via solution mixing method, by which $H_2PtCl_6 \cdot 6H_2O$, $RuCl_3 \cdot 3H_2O$, and $IrCl_3 \cdot xH_2O$ were mixed in a round-bottom flask and immersed into a thermostatic oil bath with magnetic stirring at 80 °C for 3 h, the following steps were similar with the modified microemulsion procedure mentioned above.

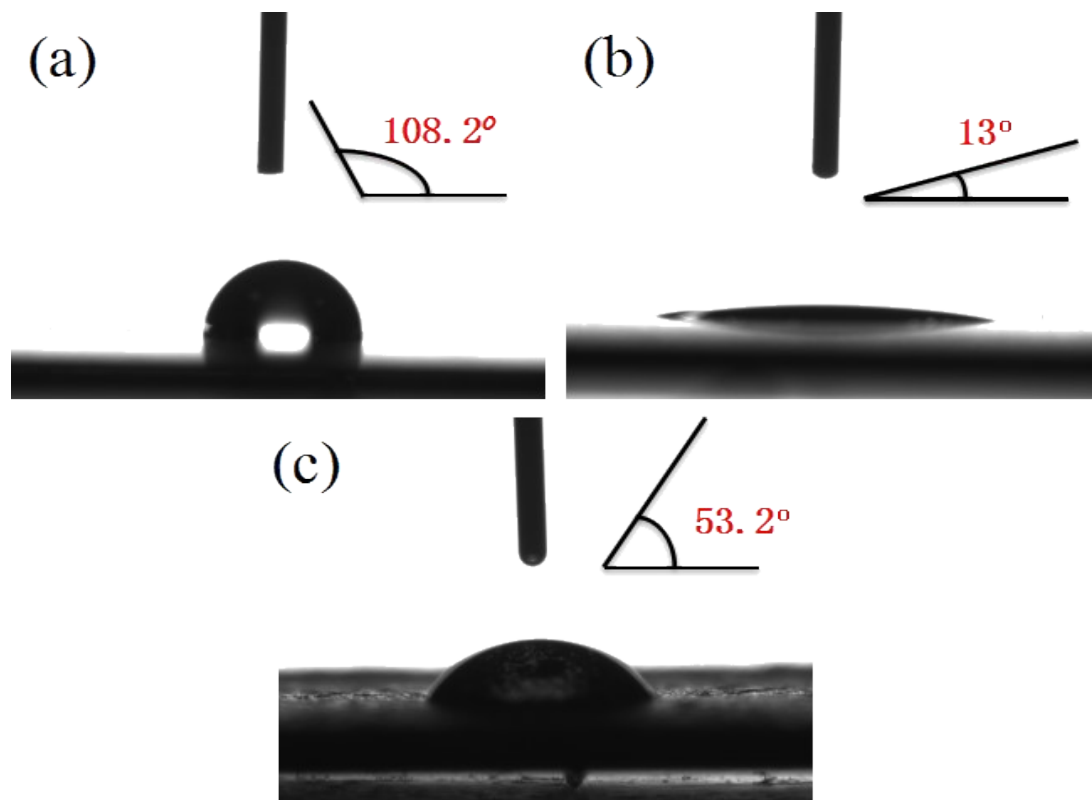


Fig. S1. Contact angle photograph of Ti/RuO₂-IrO₂@Pt (a), Ti/RuO₂-IrO₂-Pt (b), and Ti/RuO₂-IrO₂ (c).

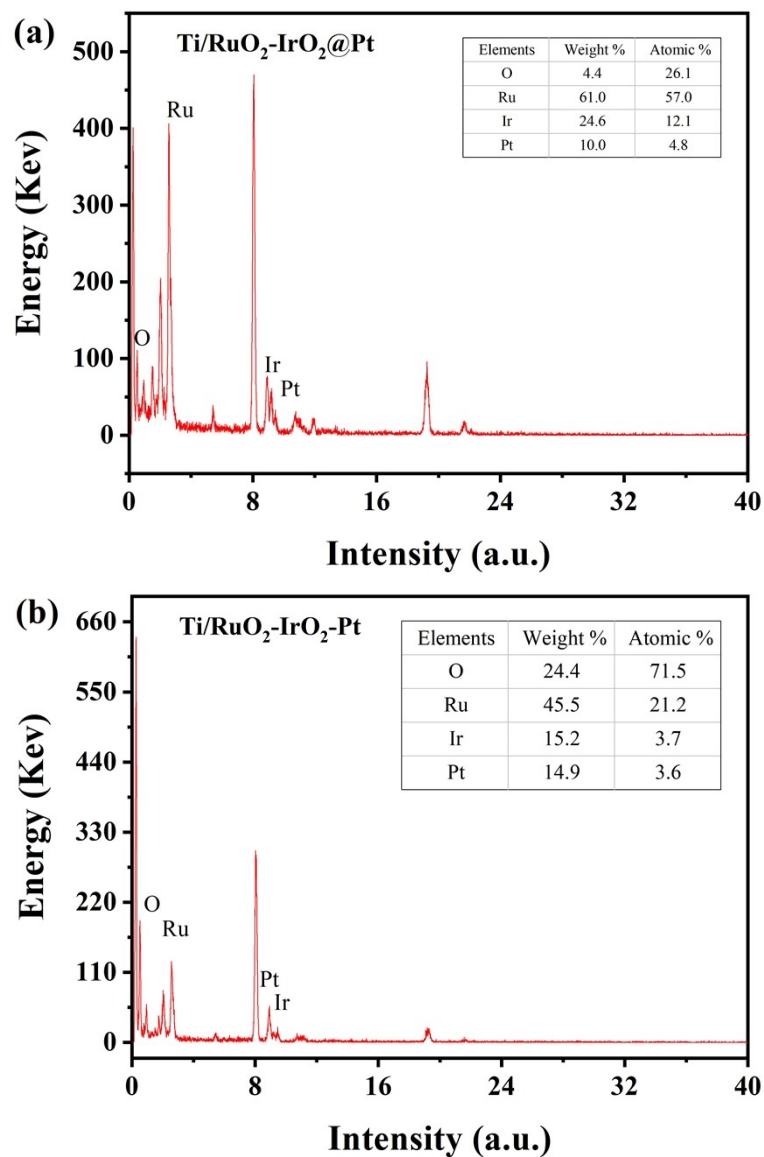


Fig. S2. The elemental composition of Ti/RuO₂-IrO₂@Pt (a) and Ti/RuO₂-IrO₂-Pt (b) electrodes.

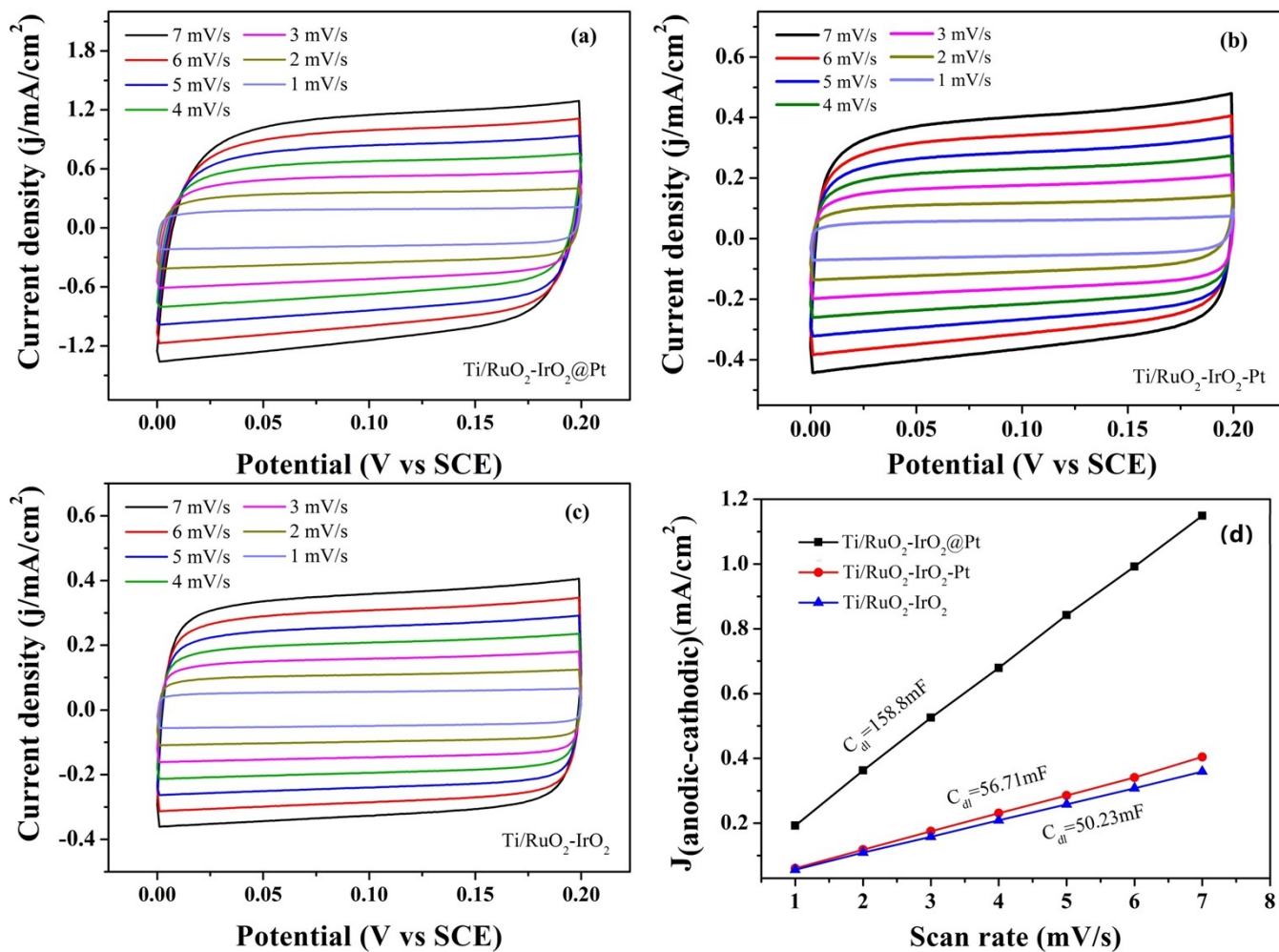


Fig. S3. CV curves of Ti/RuO₂-IrO₂@Pt (a), Ti/RuO₂-IrO₂-Pt (b), and Ti/RuO₂-IrO₂ (c) electrodes at different scanning rates. The electric double-layer capacitance diagram of these electrodes (d).

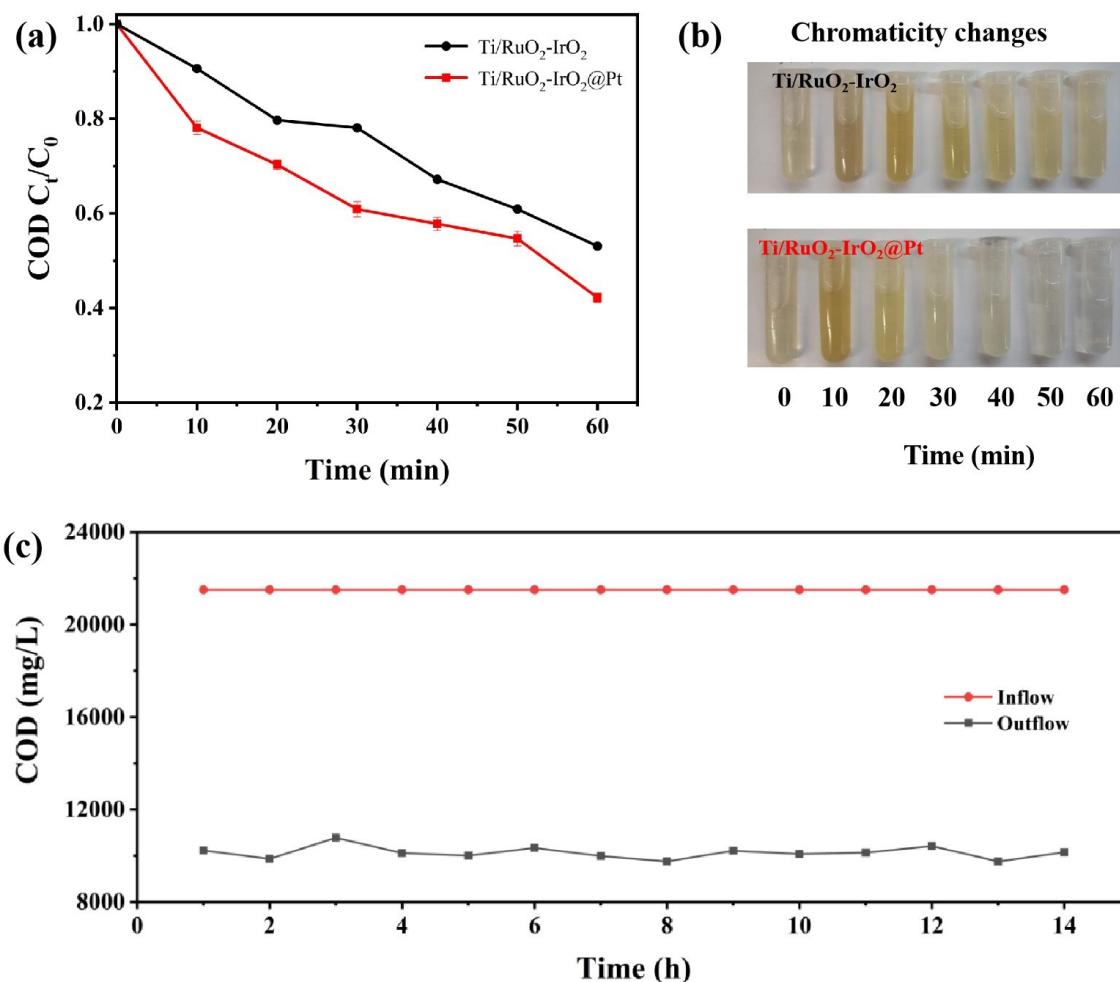


Fig. S4. Electrochemical degradation of actual pharmaceutical wastewater (obtained from Hebei pharmaceutical factory in China). (a) Chemical oxygen demand (COD) and (b) chromaticity changes with the time of electrolysis. (c) Continuous experiment by using Ti/RuO₂-IrO₂@Pt anode.

In this work, PFOA, a typical refractory organic pollutant, was selected as the target contaminant for electrochemical degradation to evaluate the electrocatalytic activity and mineralization capability of the Ti/RuO₂-IrO₂@Pt anode. As expected, Ti/RuO₂-IrO₂@Pt anode showed excellent electrocatalytic activity and mineralization ability as well as good stability during the electrochemical PFOA oxidation process. In addition, electrochemical degradation of actual pharmaceutical wastewater was also performed to further evaluate the electrocatalytic activity and stability of the Ti/RuO₂-IrO₂@Pt electrode. As shown in Fig. S4a, after 60 min of electrolysis, COD decreased from 21510 to 9077.22 mg·L⁻¹ with 57.8 %

of COD removal. Simultaneously, the chromaticity has changed significantly (Fig. S4b). Continuous electrolysis experiments also showed that Ti/RuO₂-IrO₂@Pt electrode had good stability (Fig. S4c). These facts indicate that Ti/RuO₂-IrO₂@Pt electrode is efficient for PFOA degradation and also promising for other recalcitrant pollutants degradation.

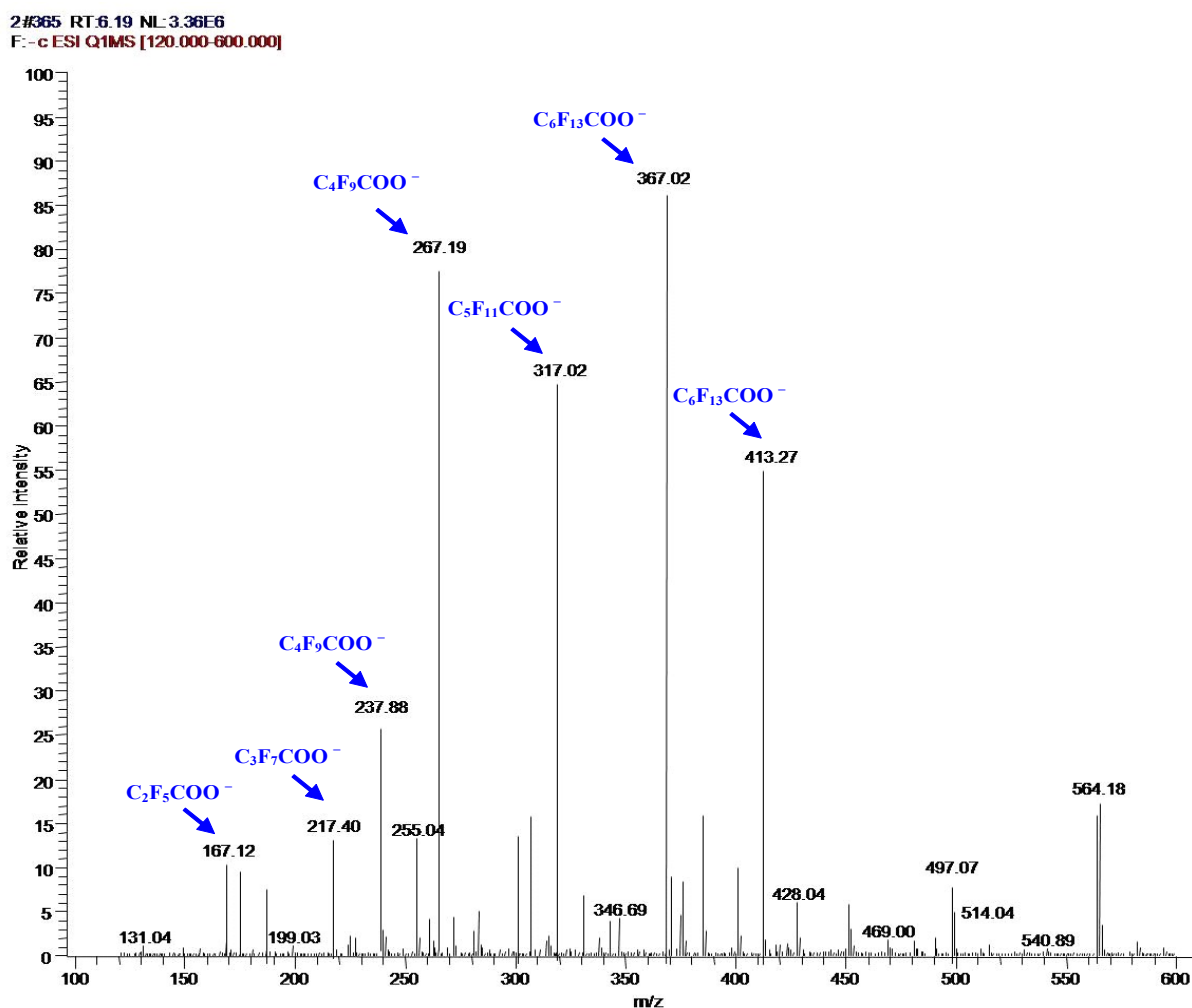


Fig. S5. ESI mass spectrum of the PFCAs by using UPLC-MS/MS.

Table S1

Comparison of service life of different DSA anodes.

Anode materials	Accelerated life test conditions	Lifetime (h)
Ti/IrO ₂ -RuO ₂ (450 °C) ¹	0.5 mol·L ⁻¹ H ₂ SO ₄ solution, 2 A·cm ⁻² current density	38
Ti/IrO ₂ -RuO ₂ ²	0.5 mol·L ⁻¹ H ₂ SO ₄ solution, 0.1 A·cm ⁻² current density, 50 °C	42
Ti/RuO ₂ -IrO ₂ -TiO ₂ ³	1 mol·L ⁻¹ H ₂ SO ₄ solution, 1 A·cm ⁻² current density	8.5
Ti/Ir _{0.3} Ru _{0.3} Ti _{0.4} O ₂ ⁴	3 mol·L ⁻¹ H ₂ SO ₄ solution, 2 A·cm ⁻² current density, 25 °C	9.8
RuO ₂ -doped Ti/IrO ₂ -ZrO ₂ ⁵	0.5 mol·L ⁻¹ H ₂ SO ₄ solution, 2 A·cm ⁻² current density	42
Ti/IrO ₂ -RuO ₂ -SiO ₂ ⁶	0.5 mol·L ⁻¹ H ₂ SO ₄ solution, 2 A·cm ⁻² current density	195
Ti/RuO ₂ -IrO ₂ (this work)	1 mol·L ⁻¹ H ₂ SO ₄ solution, 2 A·cm ⁻² current density, 40 °C	24
Ti/RuO ₂ -IrO ₂ -Pt (this work)	1 mol·L ⁻¹ H ₂ SO ₄ solution, 2 A·cm ⁻² current density, 40 °C	24.7
Ti/RuO ₂ -IrO ₂ @Pt (this work)	1 mol·L ⁻¹ H ₂ SO ₄ solution, 2 A·cm ⁻² current density, 40 °C	42.3

The accelerated life test was carried out in 1 mol·L⁻¹ H₂SO₄ solution at 40 °C under 2 A·cm⁻², which is based on the Chinese standard GB12176-90 for sodium hypochlorite generators. Compared to other methods, the conditions of the accelerated life test in our study are more demanding. Table S1 shows the comparison of service life between different anodes, and it can be found that the lifetime of Ti/RuO₂-IrO₂@Pt is significantly longer than others, confirming its super-stable nature. In addition, the value of the current density applied in the test is much higher than that employed for electro-oxidation of organics, the actual service life of the anode will be longer than that indicated in the test. The actual life is estimated with the following Eq. S1 ⁷.

$$SL_{EA}=SL_a*(j_a/j_{EA})^{1.7} \quad (S1)$$

Where SL_{EA} and j_{EA} are service life and current density of electrolysis application, SL_a and j_a are service life and current density under the accelerated life test conditions. The estimated service life of Ti/RuO₂-IrO₂@Pt anode is 6.09 years, which is highly competitive for industries.

Table S2

Comparison of PFOA degradation using DSA or BDD anodes.

Anode materials	Initial concentration (mg·L ⁻¹)	Current density (mA·cm ⁻²)	Working area (cm ²)	Time (h)	PFOA Removal (%)	TOC Removal (%)	Defluorination rate (%)
Ti/RuO ₂ -IrO ₂ @Pt	50	30.0	4.50	5.0	99.30	91.32	88.70
Ti/SnO ₂ -Sb-MnO ₂ ⁸	100	10.0	60.00	1.5	31.70	-	45.60
Ti/SnO ₂ -Sb-PbO ₂ ⁸	100	10.0	60.00	1.5	91.10	-	77.40
Ti/SnO ₂ -Sb-PbO ₂ -Ce ⁹	100	10.0	25.00	1.5	96.70	91.70	81.70
Ti/SnO ₂ -Sb ¹⁰	50	22.1	11.33	3.0	93.30	-	-
Ti/SnO ₂ -Sb-Bi ¹⁰	50	22.1	11.33	3.0	89.80	-	63.80
Ti/SnO ₂ -F ¹¹	100	20.0	30.00	0.5	99.00	92.60	84.10
BDD ¹²	100	20.0	42.00	6.0	93.00	95.00	-
BDD ¹³	10	21.4	35.05	4.0	99.50	-	50.00
BDD ¹⁴	15	50	38.00	4.0	100.00	-	70.00

“-” represents no data.

Notes and references

- 1 B. Liu, C. Wang, Y. Chen and B. Ma, *J. Electroanal. Chem.*, 2019, **837**, 175–183.
- 2 N. Yu, X. Lu, F. Song, Y. Yao and E. Han, *J. Environ. Chem. Eng.*, 2021, **9**, 105301.
- 3 W. J. de Santana Mota, G. de Oliveira Santiago Santos, A. Resende Dória, M. Rubens dos Reis Souza, L. C. Krause, G. R. Salazar-Banda, K. I. Barrios Eguiluz, J. A. López and M. L. Hernández-Macedo, *Chemosphere*, 2021, **279**, 130875.
- 4 F. Moradi and C. Dehghanian, *Prog. Nat. Sci. Mater. Int.*, 2014, **24**, 134–141.
- 5 B. Liu, S. Wang, C. Wang, Y. Chen, B. Ma and J. Zhang, *J. Alloys Compd.*, 2019, **778**, 593–602.
- 6 B. Liu, B. Ma, Y. Chen and C. Wang, *Corros. Sci.*, , DOI:10.1016/j.corsci.2020.108662.
- 7 S. Chen, Y. Zheng, S. Wang and X. Chen, *Chem. Eng. J.*, 2011, **172**, 47–51.
- 8 H. Lin, J. Niu, S. Ding and L. Zhang, *Water Res.*, 2012, **46**, 2281–2289.
- 9 J. Niu, H. Lin, J. Xu, H. Wu and Y. Li, *Environ. Sci. Technol.*, 2012, **46**, 10191–10198.
- 10 Q. Zhuo, S. Deng, B. Yang, J. Huang and G. Yu, *Environ. Sci. Technol.*, 2011, **45**, 2973–2979.
- 11 B. Yang, C. Jiang, G. Yu, Q. Zhuo, S. Deng, J. Wu and H. Zhang, *J. Hazard. Mater.*, 2015, **299**, 417–424.
- 12 A. Urriaga, C. Fernández-González, S. Gómez-Lavín and I. Ortiz, *Chemosphere*, 2015, **129**, 20–26.
- 13 J. N. Uwayezu, I. Carabante, T. Lejon, P. van Hees, P. Karlsson, P. Hollman and J. Kumpiene, *J. Environ. Manage.*, 2021, **290**, 112573.
- 14 C. E. Schaefer, C. Andaya, A. Burant, C. W. Condee, A. Urriaga, T. J. Strathmann and C. P. Higgins, *Chem. Eng. J.*, 2017, **317**, 424–432.